Nematic Fumaric Ester Derivatives and Their Electro-Optical Properties

Kohei SHIRAISHI, Kazuo SUGIYAMA,* Akihiko SAKAMOTO, and Takayuki OTSU†
Department of Industrial Chemistry, Faculty of Engineering, Kinki University, Hiro, Kure 737-01
†Department of Applied Chemistry, Faculty of Engineering, Osaka City University, Sugimoto, Sumiyoshi-ku, Osaka 558
(Received July 24, 1987)

Senven enantiotropically nematic fumaric ester derivatives, 1-[[(*E*)-3-alkoxycarbonyl)acryloyl]oxy]-4-(4-methoxyphenylazo)benzene (**1**), were prepared. The **1** compounds which have unbranched ester alkyl groups showed decreased phase-transition temperatures and narrowed nematic states with the increase in the length of the alkyl chain, while the **1** compounds with terminal branched alkyl groups decrease drastically in nematic thermal stability. From the electro-optical effect originating in the dynamical scattering at the nematic state of the **1** compounds with unbranched ester groups, it was found that both the threshold voltage (E_{thres}) of deformation and the electro-optial response time (τ_r) decrease with the decrease in the chain lengh of alkyl groups. In addition, τ_r is scarcely influenced over the wide temperature range above 12 eV·cm^{-1} of the electric field.

During the last years, interest has been increasingly devoted to liquid crystalline side-chain polymers.[1-5] This interest has been justified by the creation of novel functional materials which bind the properties of low molecular liquid crystals to macromolecules.[6,7] In these polymers, the mesogenic groups become flexible polysiloxianes[1,3] or types of vinyl backbone, such as polyacrylates[4,7] and polymethacrylates.[2] On the other hand, it has been found that dialkyl fumarates can polymerize radically to produce nonflexible rodlike polymers with a high molecular weight.[8,9] In the course of an investigation of fumaric ester derivatives with properties of liquid crystals,[10,11] a series of polymerizable fumarates, 1-[[(*E*)-3-(alkoxycarbonyl)acryloyl]oxy]-4-(4-methoxyphenylazo)benzene, **1**, were prepared in an attempt to obtain a new type of liquid crystal side-chain polymers. In this paper, we would like to report the thermal and the electro-optical properties of **1**.

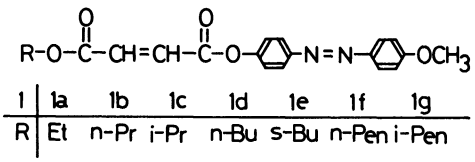

Scheme 1.

Results and Discussion

Thermal Properties. The **1** compounds were synthesized by a direct esterification of 4-(4-hydroxyphenylazo)anisole with (*E*)-3-(chloroformyl)acrylic acid alkyl esters. Alkyl groups were either ethyl(**1a**), propyl(**1b**), isopropyl(**1c**), butyl(**1d**), *s*-butyl(**1e**), pentyl(**1f**), or isopentyl(**1g**) as is shown in Scheme 1. A DSC study showed that all of the **1** compounds turned into enantiotropic liquid crystals, for showes two endothermic peaks and two exothermic peaks on heating and cooling cycles respectively. As a typical instance, the DSC curve of **1a** is shown in Fig. 1. The mesophase of **1** showed a schlieren texture and was

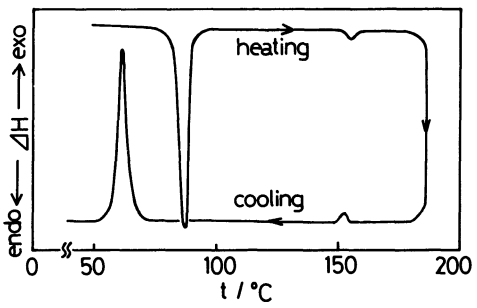

Fig. 1. DSC curve of **1a**.

Table 1. Phase Transition Temperatures and Electro-Optical Properties of **1** Compounds

Compound	R	Phase transition temperature[a]/°C	ΔT_N / °C	E_{thres}[b] / kV·cm^{-1}	Int[c] / %	τ_r[c] / ms
1a	Et	K 53.0 N 160.6 I	107.6	0.18	63	0.9
1b	*n*-Pr	K 50.0 N 153.1 I	103.1	0.28	45	1.0
1c	*i*-Pr	K 39.6 N 67.8 I	28.2	—	—	—
1d	*n*-Bu	K 27.0 N 114.4 I	87.4	0.26	80	5.7
1e	*s*-Bu	K 26.0 N 38.6 I	12.6	—	—	—
1f	*n*-Pen	K 34.0 N 118.3 I	84.3	0.40	50	4.5
1g	*i*-Pen	K 31.5 N 92.2 I	60.7	0.84	—	—

a) K, N, and I represent the crystalline, and nematic phases, and the isotropic melt respectively. b) E_{thres} was measured at T*°C(T_{N-I}−10 °C). c) Int represents the transmission intensity of the He-Ne laser. d) τ_r was measured on 16 kV·cm^{-1} of an electric field at T*°C(T_{N-I}−10 °C).

identified as a nematic phase by observation and a polarization microscopy of thin samples. The phase-transition temperature of **1** determined by DSC is compatible with the temperature obtained from the polarization microscopic and electro-optical measuremens to be described below. The results are tabulated in Table 1.

From the phase-transition temperature of **1**, the following conclusions can be drawn. Every fumarate exhibits an enantiotropically nematic phase independent of the ester alkyl groups. The phase-transition temperature is, however, strongly influenced by the structures of alkyl groups. In the case of unbranched alkyl groups (**1a**, **1b**, **1d**, **1f**), with an increase in the length of the alkyl chain the nematic-isotropic melt transition point loweres and the nematic state is narrowed. Comparing the unbranched type (**1b**, **1d**, **1f**), with the branched type (**1c**, **1e**, **1g**), the latter samples show lower transition temperatures. This suggests that the bulkiness of an alkyl group decreases the attractive interaction between the molecules; that is, a branching of a terminal alkyl group decreases the nematic thermal stability.[12,13] Especially, **1c** and **1e** with a methyl group at the α-position in the alkyl group are found to exhibit an extremely low nematic-isotropic melt transition. This explains the destruction of the molecular order by the methyl group at the α-position.[14]

Electro-Optical Properties. In order to obtain basic data for such practical uses as optical switching and display devices, electro-optical measurements were carried out for **1a**, **1b**, **1d**, and **1f** as follows. The sample cell was set in the optical path of a He–Ne laser(632.8 nm), and the change in the transmission with the application of an electric field was monitored by means of a photodiode.[15] As a typical example, the transmission intensity of the He–Ne laser through the **1a** cell on cooling cycles is shown in Fig. 2. The lines in Fig. 2 alternately indicate, the presence or absence of the dependence of the transmission intensities of the He–Ne laser through the cell on the applied voltage. When no voltage is applied, the transmission intensity decreases abruptly because of characteristic nematic light scattering just after the phase transition from the isotropic melt to the nematic phase at 160.6 °C, and then it gradually increases up to 63% of the original intensity by forming a stable nematic phase. On the other hand, upon the application of a voltage, the transmission intensity is zero over the nematic range of **1a** because of dynamical scattering caused by the d.c. current. The extent of these changes in the transmission intensity upon the application of an electric field is evaluated as a contrast in liquid-crystal displays. The threshold voltage of the observed deformation was measured at a definite temperature, T^* °C(T^*= T_{N-I}−10 °C), the results are listed in Table 1. Liquid crystals with a long alkyl group show a considerably higher threshold voltage of dynamical scattering. This is believed to be due to the higher viscosity of the nematic phase of **1** with the longer alkyl groups. The electro-optical response time (τ_r) of the decrease in the transmission caused by the voltage application was

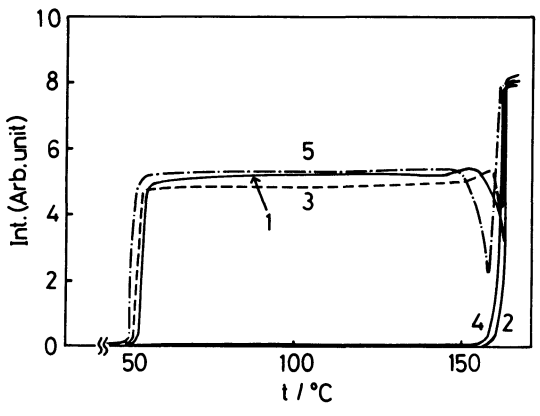

Fig. 2. Transmission intensities of a He–Ne laser for **1a** cell thickness; 50 μm, 1; (OFF), 2; 20 V(ON), 3; (OFF), 4; 40 V(ON), 5; (OFF).

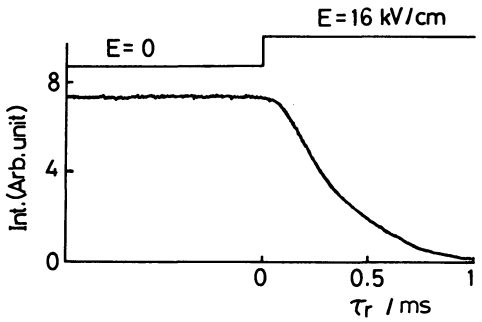

Fig. 3. Electro-optical response time(τ_r) in the nematic phase of **1a** at 16 kV·cm^{-1}.

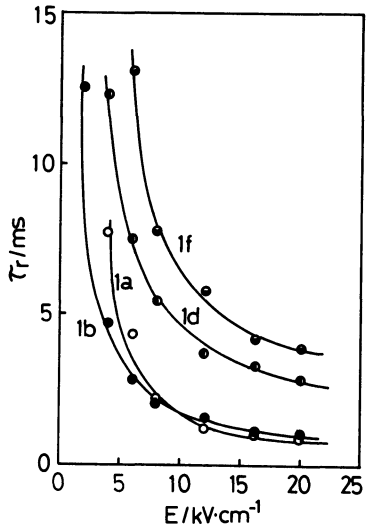

Fig. 4. Effect of electric field (E) on electro-optical response time (τ_r) for **1** at T^*°C(T^*=T_{N-I}−10 °C).

then measured over the voltage range from 5V (electric field, E=1 kV·cm^{-1}) to 100 V (E=20 kV·cm^{-1}) at T^* °C. In the case of **1a**, τ_r at 150.6 °C with E=16 kV·cm^{-1} is shown in Fig. 3. τ_r is the time taken to reach the stage of a transmission intensity decrease of 10%. τ_r for **1a** is, then, found to be 0.9 ms.

τ_r was also measured for other samples in a similar manner, by changing the applied voltage. The relation of τ_r and, the electric field applied at T^* °C is shown in Fig. 4. This figure shows that an increase in the applied voltage results in a faster optical response time, while an increase in the length of alkyl chain in **1** results in a slower response time. In order to clarify the effect of the electric field on the optical response time, τ_r was plotted on log-log graph paper as a function of the electric field, as is shown in Fig. 5.

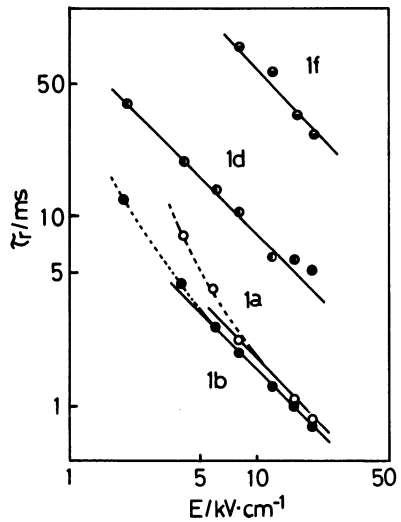

Fig. 5. Log-log plots of electro-optical response time (τ_r) and electric field (E) for **1** at T^*°C(T^*=T_{N-I}−10 °C).

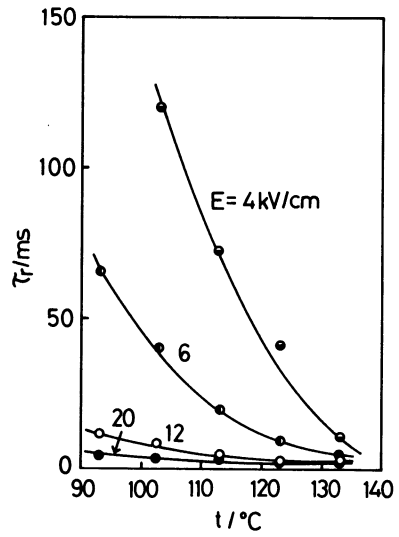

Fig. 6. Effect of temperature on electro-optical response time (τ_r) at various electric fields (E).

Since the slope of the lines is approximately −1, the τ_r of these liquid crystals is found to be proportional to the reciprocal of the electric field applied.[16] In the cases of **1a** and **1b** the plots deviate from the lines at somewhat lower electric fields. The reason for this phenomenon is now under consideration.

The effect of the temperature on τ_r was also studied by changing the applied voltage. As a typical example, the relationship between τ_r and the temperature for **1b** is shown in Fig. 6. It is found that τ_r is scarcely influenced over the wide temperature range above E=12 eV·cm^{-1} of the electric field. The transmission intensities of a He-Ne laser, τ_r, for **1a**, **1b**, **1d**, and **1f** are summarized in Table 1. Both a short response time and a clear contrast attributable to the change of transmission are realized with these liquid crystals. In general, the most desirable properties of a liquid crystal to be used as a material for display devices are as follows: i) the phase-transition temperature is low, and the temperature range of its mesophase is wide; ii) the optical response can occur at a low electric field and is accompanied by a high contrast; iii) the response times of rise and decay show an approximately exponential decrease with the temperature, and iv) the threshold voltage for the electric-field effect is proportional to the reciprocal of dielectric anisotropy. The liquid crystals obtained in this work can, therefore, be applied practically as display devices. The polymerization of **1** is now under investigation.

Experimental

Preparation of 1. 4-(4-Hydroxyphenylazo)anisole was obtained from the diazotization of *p*-anisidine and coupling with phenol according to the method used in the preparation of 4-(4-hydroxyphenylazo)benzonitrile.[17] 4-(4-Hydroxyphenylazo)anisole was dissolved in 300 mL of freshly distilled chloroform and 130 mmol of triethylamine. Then a trace of 1,4-benzoquinone was stirred in, the solution was cooled at 0 °C, and a 80-mmol portion of (*E*)-3-(chloroformyl)acrylic acid alkyl esters was dropped into the solution. After stirring for 2 h at 60 °C, ca. 200 mL of water was added to the reaction mixture. The chloroform layer was then washed with water and evaporated to dryness, and the residue was recrystallized from ethanol. **1** was chracterized by IR, ^{1}H NMR, and elemental analysis as follows:

1a (R=CH_3CH_2–): 65.6% yield; ^{1}H NMR ($CDCl_3$) δ= 1.26—1.66 (t, 3H, CH_3CH_2–), 4.00 (s, 3H, CH_3O–), 4.30—4.82 (q, 2H, CH_3CH_2–), 7.34 (s, 2H, –CH=CH–), 7.88—8.62 (q, 8H, Aromatic): $C_{19}H_{18}O_5N_2$ (354.36); Found C, 64.3; H, 5.1; N, 7.7%. Calcd for C, 64.40; H, 5.12; N, 7.91%.

1b (R=$CH_3CH_2CH_2$–): 67.2% yield; ^{1}H NMR ($CDCl_3$) δ=0.90—1.40 (t, 3H, $CH_3CH_2CH_2$–), 1.62—2.12 (sex, 2H, $CH_3CH_2CH_2$–), 4.04 (s, 3H, CH_3O–), 4.30—4.68 (t, 2H, $CH_3CH_2CH_2$–), 7.36 (s, 2H, –CH=CH–), 7.54—8.56 (q, 8H, Aromatic): $C_{20}H_{20}O_5N_2$ (368.39); Found C, 65.3; H, 5.4; N, 7.4%. Calcd for C, 65.21; H, 5.47; N, 7.64%.

1c (R=$(CH_3)_2CH$–): ^{1}H NMR ($CDCl_3$) δ=1.34, 1.40 (s, s,

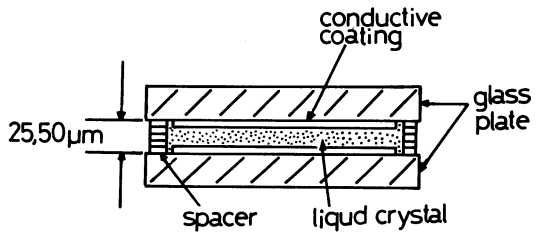

Fig. 7. Schematic representation of sandwiched cell for electro-optical measurement.

6H, $(CH_3)_2CH$-), 4.04 (s, 3H, CH_3O-), 5.16—5.52 (pent, 1H, $(CH_3)_2CH$-), 7.34 (s, 2H, -CH=CH-), 7.50—8.68 (q, 8H, Aromatic): $C_{20}H_{20}O_5N_2$ (368.39): Found C, 65.3; H, 5.4; N, 7.4 Calcd for C, 65.21; H, 5.47; N, 7.64%.

1d (R=$CH_3CH_2CH_2CH_2$-): 57.1% yield; ^1H NMR ($CDCl_3$) δ=0.92—1.06 (t, 3H, $CH_3CH_2CH_2CH_2$-), 1.32—2.06 (m, 4H, $CH_3CH_2CH_2CH_2$-), 3.98 (s, 3H, CH_3O-), 4.32—4.80 (t, 2H, $CH_3CH_2CH_2CH_2$-), 7.34 (s, 2H, -CH=CH-), 7.50—8.78 (q, 8H, Aromatic): $C_{21}H_{22}O_5N_2$ (382.42); Found C, 65.9; H, 5.8; N, 7.7%. Calcd for C, 65.96; H, 5.80; N, 7.33%.

1e (R=$CH_3CH_2(CH_3)CH$-): 74.5% yield; ^1H NMR ($CDCl_3$) δ=0.92-1.04 (m, 3H, CH_3-), 1.32-1.36 (d, 3H, CH_3-), 1.54-2.02 (m, 2H, $-CH_2$-), 4.10 (s, 3H, CH_3O-), 5.02-5.48 (m, 1H, -CH-), 7.34 (s, 2H, -CH=CH-), 7.50-8.80 (q, 8H, Aromatic): $C_{21}H_{22}O_5N_2$ (382.42): Found C, 66.0; H, 5.8; N, 7.1%. Calcd for C, 65.96; H, 5.80; N, 7.33%.

1f (R=$CH_3(CH_2)_3CH_2$-): 70.7% yield; ^1H NMR ($CDCl_3$) δ=0.86-1.20 (t, 3H, CH_3-), 1.32—2.12 (m, 6H, $CH_3(CH_2)_3CH_2$-), 4.04 (s, 3H, CH_3O-), 4.34—4.66 (t, 2H, $CH_3(CH_2)_3CH_2$-), 7.36 (s, 2H, -CH=CH-), 7.54—8.56 (q, 8H, Aromatic): $C_{22}H_{24}O_5N_2$ (395.42): Found C, 66.4; H, 6.1; N, 7.2%. Calcd for C, 66.65; H, 6.10; N, 7.70%.

1g (R=$(CH_3)_2CHCH_2CH_2$-): 75.2% yield; ^1H NMR ($CDCl_3$) δ=0.98, 1.04 (s, s, 6H, $(CH_3)_2CHCH_2CH_2$-), 1.54—2.14 (m, 3H, $(CH_3)_2CHCH_2CH_2$-), 4.06 (s, 3H, CH_3O-), 7.36 (s, 2H, -CH=CH-), 7.54-8.64 (q, 8H, Aromatic): $C_{22}H_{24}O_5N_2$ (396.42): Found C, 66.4; H, 6.1; N, 7.1%. Calcd for C, 66.64; H, 6.10; N, 7.07%.

Measurements. The ^1H NMR measurements were carried out with a 100-MHz Jeol JNM-MH100 spectrometer. The phase-transition temperature were determined by means of differential scanning calorimetry, using a Rigaku Thermoflex apparatus DSC-8230B, with almost the same heating and cooling rates (10 K·min^{-1}). The sample sizes varied from 5 to 10 mg.

Microscopic investigations were performed by means of an Olympus microscope, with the temperature of the sample controlled by the heating stage. The thin samples were sandwiched between two glass slides whose surfaces had been unidirectionally rubbed with cotton wool to obtain a homogeneous alignment.[18-20] The spacing between top and bottom glass plates was 25 μm, with a stretched polyester film used as the spacer material. The samples were studied at both decreasing and increasing temperatures.

The sandwiched cell used in electro-opotical measurements is schematically illustrated in Fig. 7. The surfaces of the glass plates were coated with a transparent conductive material(InO_2); the surface resistance was about 100 ohms·square^{-1}. The spacings between top and bottom glass plates was 50 μm. A He-Ne laser(wavelength; 632.8 nm, output power; 1 mW) was used as the light source for the measurements of the transmission intensity. The incident light was performed with both an attenuator and a slit. The transmission lights were measured using a photomultiplier and were calculated using a microcomputer (NEC-9801).

References

1) H. Pranoto, F-J. Bormuth, and W. Haase, *Makromol. Chem.*, **187**, 2453 (1986).

2) C. Boeffel, H. W. Spiess, B. Hisgen, H. Ringsdorf, H. Ohm, and R. G. Kirste, *Makromol. Chem. Rapid Commun.*, **7**, 777 (1986).

3) G. W. Gray, D. Lacey, G. Nestor, and M. S. White, *Makromol. Chem. Rapid Commun.*, **7**, 71 (1986).

4) P. Keller, *Macromolecules*, **20**, 462 (1987).

5) M. Eich, J. H. Wendorff, B. Reck, and H. Ringsdorf, *Makromol. Chem., Rapid Commun.*, **8**, 59 (1987).

6) H. J. Coles and R. Simon, *Polymer*, **26**, 1801 (1985).

7) G. R. Mitchell, F. J. Davis, and A. Ashman, *Polymer*, **28**, 639 (1987).

8) T. Otsu and K. Shiraishi, *Macromolecules*, **18**, 1795 (1985).

9) T. Otsu, A. Tatsumi, and A. Matsumoto, *J. Polym. Sci., Polym. Lett. Ed.*, **24**, 113 (1986).

10) K. Sugiyama, A. Sakamoto, Y. Murata, K. Shiraishi, and T. Otsu, *Nippon Kagaku Kaishi*, **1987**, 1064.

11) K. Shiraishi, A. Sakamoto, and K. Sugiyama, *Chem. Express* **2**, 475 (1987).

12) G. W. Gray and K. J. Harrison, *Symp. Faraday Soc.*, **5**, 54 (1971).

13) G. W. Gray and K. J. Harrison, *Mol. Cryst. Liq. Cryst.*, **13**, 37 (1971).

14) Y. Matsunaga and N. Miyajima, *Bull. Chem. Soc. Jpn.*, **57**, 1413 (1984).

15) S. Kishio, M. Ozaki, K. Yoshino, and A. Sakamoto, *Mol. Cryst. Liq. Cryst.* in press.

16) E. Jakeman and E. P. Raynes, *Phys. Lett., A*, **39**, 69 (1972).

17) H. Ringsdorf and H.-W. Schmidt, *Makromol. Chem.*, **185**, 1327 (1984).

18) F. J. Kahn, G. N. Taylor, and H. Schonborn, *Proc. IEEE.*, **61**, 823 (1976).

19) R. W. Gurtler and J. W. Casey, *Mol. Cryst. Liq. Cryst.*, **35**, 275 (1976).

20) K. Kuroda and I. Tsunoda, 8th International Liq. Cryst. Conf. J-4p (1980).